



NRC Publications Archive Archives des publications du CNRC

Transient model for coupled heat, air and moisture transfer through multilayered porous media

Tariku, F.; Kumaran, M. K.; Fazio, P.

This publication could be one of several versions: author's original, accepted manuscript or the publisher's version. /
La version de cette publication peut être l'une des suivantes : la version prépublication de l'auteur, la version
acceptée du manuscrit ou la version de l'éditeur.

For the publisher's version, please access the DOI link below. / Pour consulter la version de l'éditeur, utilisez le lien
DOI ci-dessous.

Publisher's version / Version de l'éditeur:

<http://dx.doi.org/10.1016/j.ijheatmasstransfer.2010.03.024>

International Journal of Heat and Mass Transfer, 53, pp. 3035-3044, 2010-05-01

NRC Publications Record / Notice d'Archives des publications de CNRC:

<http://nparc.cisti-icist.nrc-cnrc.gc.ca/npsi/ctrl?lang=en>

<http://nparc.cisti-icist.nrc-cnrc.gc.ca/npsi/ctrl?lang=fr>

Access and use of this website and the material on it are subject to the Terms and Conditions set forth at

http://nparc.cisti-icist.nrc-cnrc.gc.ca/npsi/jsp/nparc_cp.jsp?lang=en

READ THESE TERMS AND CONDITIONS CAREFULLY BEFORE USING THIS WEBSITE.

L'accès à ce site Web et l'utilisation de son contenu sont assujettis aux conditions présentées dans le site

http://nparc.cisti-icist.nrc-cnrc.gc.ca/npsi/jsp/nparc_cp.jsp?lang=fr

LISEZ CES CONDITIONS ATTENTIVEMENT AVANT D'UTILISER CE SITE WEB.

Contact us / Contactez nous: nparc.cisti@nrc-cnrc.gc.ca.





Transient model for coupled heat, air and moisture transfer through multilayered porous media

NRCC-53317

Tariku, F.; Kumaran, M.K.; Fazio, P.

May 2010

A version of this document is published in / Une version de ce document se trouve dans:
International Journal of Heat and Mass Transfer, 53, pp. 3035-3044, May 01,
2010, DOI: [10.1016/j.ijheatmasstransfer.2010.03.024](http://dx.doi.org/10.1016/j.ijheatmasstransfer.2010.03.024)

The material in this document is covered by the provisions of the Copyright Act, by Canadian laws, policies, regulations and international agreements. Such provisions serve to identify the information source and, in specific instances, to prohibit reproduction of materials without written permission. For more information visit <http://laws.justice.gc.ca/en/showtdm/cs/C-42>

Les renseignements dans ce document sont protégés par la Loi sur le droit d'auteur, par les lois, les politiques et les règlements du Canada et des accords internationaux. Ces dispositions permettent d'identifier la source de l'information et, dans certains cas, d'interdire la copie de documents sans permission écrite. Pour obtenir de plus amples renseignements : <http://lois.justice.gc.ca/fr/showtdm/cs/C-42>



National Research
Council Canada

Conseil national
de recherches Canada

Canada 

Transient Model for Coupled Heat, Air and Moisture Transfer through Multilayered Porous Media

Fitsum Tariku¹

British Columbia Institute of Technology, 3700 Willingdon Ave., Burnaby,
British Columbia, Canada V5G 3H2

Kumar Kumaran

National Research Council, Institute for Research in Construction, 1200 Montreal rd., Ottawa,
Ontario, Canada, K1A 0R6

Paul Fazio

Concordia University, 1455 de Maisonneuve Blvd. West, Montreal,
Quebec, Canada, H3G 1M8

Abstract

Most building materials are porous, composed of solid matrix and pores. The time varying indoor and outdoor climatic conditions result heat, air and moisture (HAM) transfer across building enclosures. In this paper, a transient model that solves the coupled heat, air and moisture transfer through multilayered porous media is developed and benchmarked using internationally published analytical, numerical and experimental test cases. The good agreements obtained with the respective test cases suggest that the model can be used to assess the hygrothermal performance of building envelope components as well as to simulate the dynamic moisture absorption and release of moisture buffering materials.

Keywords: transient HAM, moisture, hygrothermal, building envelope

¹ Corresponding author, email: Fitsum_tariku@bcit.ca

<p><u>Nomenclature</u></p> <p>Cp_a specific heat capacity of air (J/(K·kg))</p> <p>Cp_v specific heat capacity of water vapor (J/(K·kg))</p> <p>Cp_l specific heat capacity of liquid water (J/(K·kg))</p> <p>D_l liquid conductivity (s)</p> <p>g acceleration due to gravity (m/s²)</p> <p>h_{fg} latent heat of condensation/evaporation (J/kg)</p> <p>j_v vapor diffusion flux (kg/(m²·s))</p> <p>j_l liquid conduction flux (kg/(m²·s))</p> <p>k_a airflow coefficient (s)</p> <p>\dot{m}_c moisture condensation/evaporation rate (kg/s)</p> <p>M molar mass of water (0.01806 kg/mol)</p> <p>P_v vapor pressures (Pa)</p> <p>P_s suction pressures (Pa)</p> <p>\hat{P} saturated vapor pressure (Pa)</p> <p>P_{atm} atmospheric pressure (Pa)</p> <p>R universal gas constant (8.314 J/(K· mol))</p>	<p>T temperature (°C)</p> <p>V air velocity (m/s)</p> <p>Y_v mass fraction of water vapor (-)</p> <p>Y_l mass fraction of liquid water (-)</p> <p>w moisture content (kg/m³)</p> <p><u>Greek symbols</u></p> <p>δ_v vapor permeability (s)</p> <p>Θ sorption capacity (kg/m³)</p> <p>μ air dynamic viscosity (kg/(m·s))</p> <p>ρ_a density of air (kg/m³)</p> <p>ρ_w density of water (kg/m³)</p> <p>ρ_m density of material (kg/m³)</p> <p>ϕ relative humidity (-)</p> <p>ω absolute humidity (kg/kg-air)</p>
--	---

1. INTRODUCTION

The three aspects of building design: durability, indoor humidity level, and energy performance are interrelated and have to be considered simultaneously as part of an optimized building design. The thermal and moisture dynamic response of building enclosures have strong impact on the humidity condition of the indoor space and energy consumption of the building. To accurately capture the influence of the building enclosure on the indoor environment and HVAC systems, a transient heat, air and moisture (HAM) transfer model that handles the coupled heat, air and moisture transfer phenomena through building enclosure is essential. The model enables dealing with the three important aspects of whole building hygrothermal analysis.

The first aspect relates to assessing the degree of moisture buffering effects of interior lining materials. El Diasty et al. [1] and Jones [2] suggested that as much as one third of the moisture release into the indoor air could be absorbed by interior moisture buffering materials. These materials have a potential of modulating the indoor humidity level [3-4], especially in cases where the ventilation rate is low [1,5]. Thus, obtaining a detailed account of the dynamic moisture absorption and release of moisture buffering materials is a crucial step in more accurately predicting the indoor humidity level and fluctuation over time.

Another advantage of having a detailed transient HAM model as one of the basic building blocks of whole building hygrothermal model is that it enables more accurately capturing the potential moisture release from the building enclosure to the indoor space. In fact, Christian [6] stated that moisture sources from construction (e.g. initial moisture content of concrete), and from wet soil through foundation walls and floor slab could dominate all internal moisture sources. Similarly, TenWolde [7] recently emphasized the importance of quantification of the moisture release from foundation slabs when calculating indoor humidity levels. Christian [6]

estimated a total of 200 liters moisture release by an average house constructed with lumber having an average of 19% moisture content; and 90 liters of water release per cubic meter of concrete used during the construction. The effect of these significant moisture releases to the indoor space and the moisture exchange between outdoor and indoor environments, including the wind-driven rain load, on the overall hygrothermal performance of a building can be more effectively estimated and understood using a transient coupled HAM model [8-9].

A third advantage of the use of a transient HAM model when conducting whole building performance analysis is that it yields a better estimation of energy demand for heating or cooling of a building. This is possible due to the fact a transient HAM model takes into account the effect of moisture in the heat transfer through building enclosures. Usually energy simulation models ignore the moisture effect when conducting the thermal analysis [10], and use constant thermal storage and transport (thermal conductivity and heat capacity, respectively) property values despite the fact that these properties can be strongly dependent on moisture content. For example, as the moisture content of wood increases to 10% [11] its corresponding thermal storage capacity increases by 30% as compared to its dry state; likewise, the thermal conductivity of lime silica brick increases more than twice as the moisture content increase to full saturation [12]. This implies that arbitrary choices of values for the thermal transport and storage property of materials may result in an incorrect prediction of heat flux through building enclosure as demonstrated in Hagentoft's [13] simple calculation of heat fluxes with and without moisture in a structure. Other important effects of moisture on energy calculations, quite often omitted in whole building energy analysis tools, are the latent heat transfer across the building enclosure and the local heating and cooling effects that are generated within the structure due to moisture phase changes (condensation and evaporation, respectively). In this paper, details on

the development and validation of a heat and moisture transfer model that takes into account critical issues such as moisture buffering effects, moisture sources and the effects of moisture on heat transfer is presented.

2. MATHEMATICAL MODELS FOR COUPLED HEAT, AIR AND MOISTURE TRANSFER THROUGH POROUS MEDIA

Most building materials are porous, and composed of solid matrices and pores. In the pores, moisture can exist in any of the three thermodynamic states of matter, i.e. the gas (vapor), liquid and solid (ice) states. However, moisture movement is possible only in the vapor and liquid states. The main mechanisms of moisture transfer can be by vapor diffusion, capillary suction or a combination of both, depending up on the moisture content of the material. Materials have unique equilibrium moisture content characteristic curve that covers the hygroscopic and capillary water regions. These regions are commonly referred to as sorption isotherm and water retention curves respectively, for which a typical equilibrium moisture content characteristic curve is shown in Figure 1. In the hygroscopic region, the pores are mainly filled with water vapor (Figure 2 (a)) and consequently, the moisture transport is mainly by vapor diffusion. Liquid water transport is possible for the case where the pores are filled with liquid water (Figure 2 (b)). This flow mechanism is very active in the capillary water region, where the relative humidity is over 95%. Both vapor and liquid transport can co-exist in the higher end of the hygroscopic region, as illustrated in Figure 2 (c). In this region, both vapor diffusion and capillary suction are active in large and small pores, respectively. Vapor diffuses in the open pores and condenses on the capillary meniscus, whereas on the other end of the meniscus, water

evaporates into the next open pore space. This implies that the diffusion path is reduced, resulting in an increase in the rate of moisture.

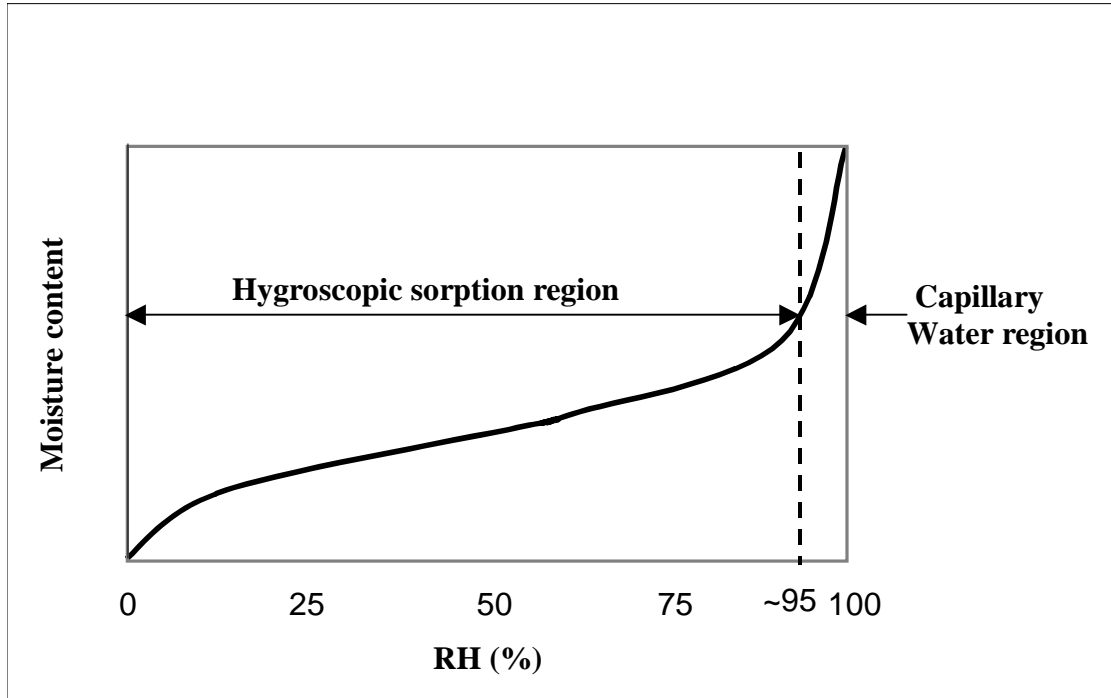


Figure 1 Equilibrium moisture content profile of a typical material.

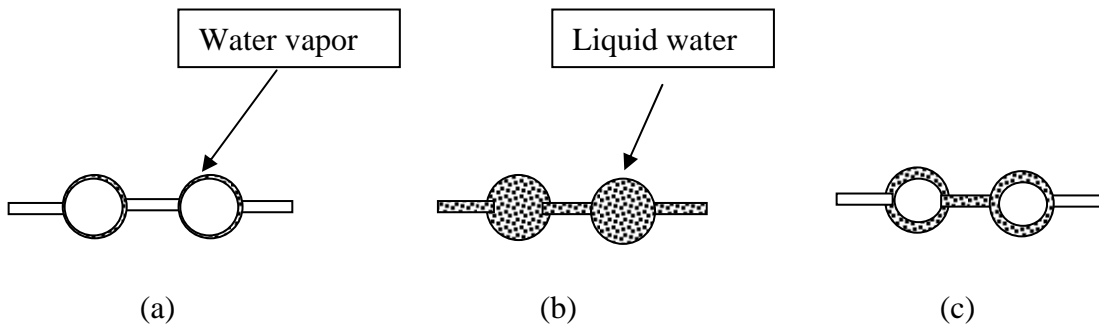


Figure 2 Moisture in idealized pores [14] (a) pores in hygroscopic region, (b) pores in capillary water region (c) pores in high end of hygroscopic region

2.1. Moisture transfer

The basic governing equation for moisture flow through a porous medium, given by Equation [3], can be derived by adding the species conservation equations of water vapor (Equation [1]) and liquid water (Equation [2]).

$$\rho_m \frac{\partial Y_v}{\partial t} + \rho_m \operatorname{div}(VY_v) + \operatorname{div}(j_v) = -\dot{m}_c \quad [1]$$

+

$$\rho_m \frac{\partial Y_l}{\partial t} + \operatorname{div}(j_l) = \dot{m}_c \quad [2]$$

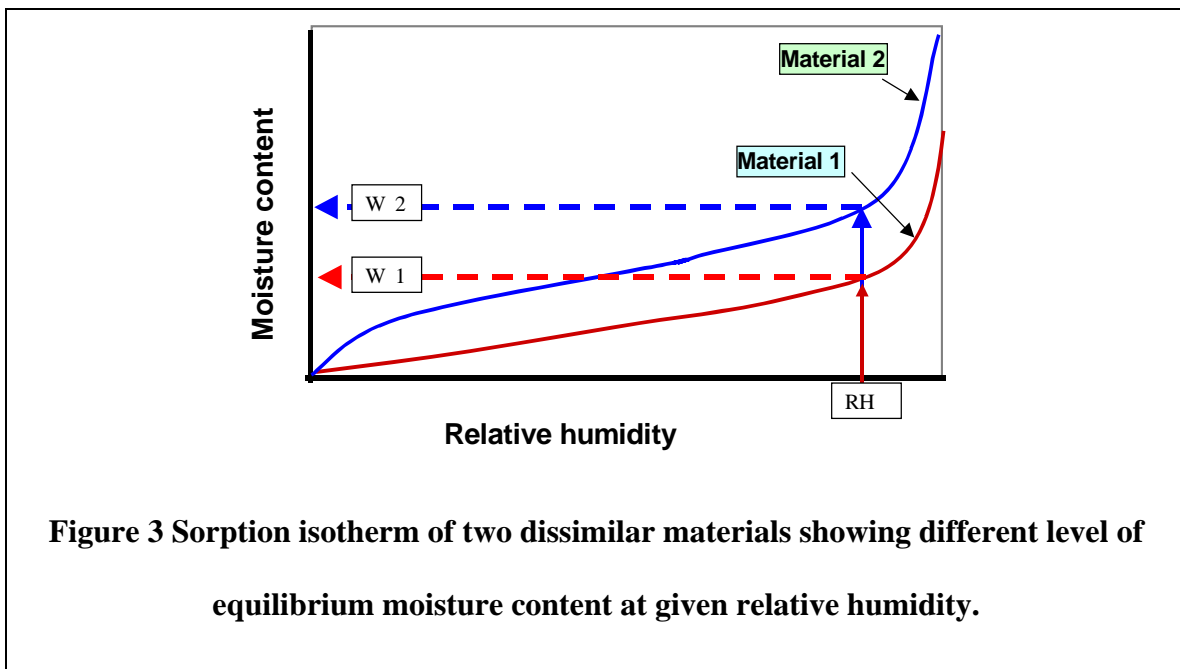
gives

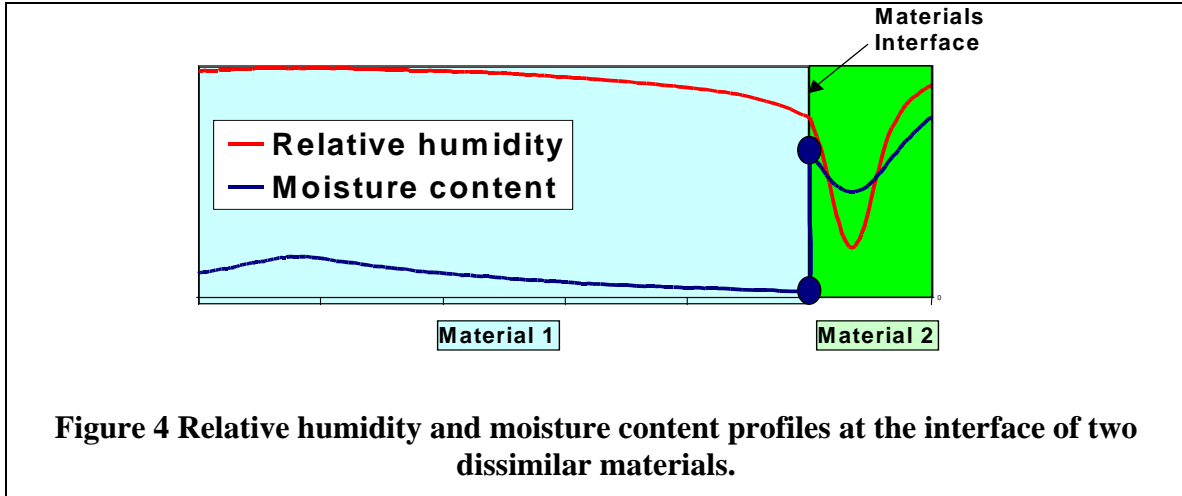
$$\rho_m \left(\frac{\partial Y_v}{\partial t} + \frac{\partial Y_l}{\partial t} \right) + \rho_m \operatorname{div}(VY_v) + \operatorname{div}(j_v) + \operatorname{div}(j_l) = 0 \quad [3]$$

Expressing the transient term in terms of moisture content $\left(\text{i.e., } \rho_m \left(\frac{\partial Y_v}{\partial t} + \frac{\partial Y_l}{\partial t} \right) = \frac{\partial w}{\partial t} \right)$, and rewriting the vapor mass fraction in the second term in terms of the humidity ratio, and substituting the vapor diffusion and liquid conduction fluxes (in the third and fourth terms, respectively) with Fick's and Darcy's law, respectively, yields moisture balance Equation [4].

$$\frac{\partial w}{\partial t} + \operatorname{div}(\rho_a V \omega) + \operatorname{div} \left(-\delta_v \frac{\partial P_v}{\partial x_i} \right) + \operatorname{div} \left(D_l \left(\frac{\partial P_s}{\partial x_i} + \rho_w g \right) \right) = 0 \quad [4]$$

The moisture balance equation (Equation [4]) is comprised of various moisture driving potentials, specifically: w , ω , P_v and P_s . These driving potentials, and the associated gradients, can be expressed in terms of a single flow potential. The chosen flow potential in this work is relative humidity (ϕ) since it is continuous at the interface of two layers of materials having different moisture storage properties (sorption and moisture retention), in contrary to moisture content, which is discontinuous. This is illustrated in Figure 3 and Figure 4 as follow: the relative humidity at the contact surfaces of material 1 and material 2 are equal since the vapor pressure and temperature are continuous at the interface. However, as shown in Figure 3, the equilibrium moisture contents of the respective contacting surfaces are different (W_1 and W_2). Consequently, as illustrated in Figure 4 at the interface the moisture content profile becomes discontinuous as it jumps from W_1 to W_2 . Relative humidity, on the other hand, is continuous throughout the computational domain.





Consequently, all terms in the moisture balance equation (Equation [4]) are mathematically transformed using relative humidity as a driving potential as follow:

a) **Transient term:** $\left(\frac{\partial w}{\partial t}\right)$

$$\frac{\partial w}{\partial t} = \frac{\partial w}{\partial \phi} \cdot \frac{\partial \phi}{\partial t} \quad \Theta = \frac{\partial w}{\partial \phi} \quad \text{Where } \Theta = \frac{\partial w}{\partial \phi} \text{ is the sorption capacity}$$

(Slop of sorption-moisture retention curve)

$$\frac{\partial w}{\partial t} = \Theta \frac{\partial \phi}{\partial t} \quad [4A]$$

b) **ω in the Vapor convection term**

$$\omega = \frac{0.622 \cdot P_v}{P_{atm} - P_v}; \quad P_{atm} - P_v \approx P_{atm}; \quad P_v = \hat{P}(T) \cdot \phi$$

$$\omega = \frac{0.622 \cdot \hat{P}(T) \cdot \phi}{P_{atm}}; \quad C_c = \frac{0.622}{P_{atm}}$$

where P_{atm} is atmospheric pressure

$$\omega = C_c \hat{P} \cdot \phi \quad [4B]$$

c) Vapor pressure gradient in the vapor diffusion term: $\left(\frac{\partial P_v}{\partial x_i} \right)$

$$\frac{\partial P_v}{\partial x_i} = \frac{\partial (\hat{P}(T) \cdot \phi)}{\partial x_i} = \phi \frac{\partial \hat{P}(T)}{\partial x_i} + \hat{P} \frac{\partial \phi}{\partial x_i}$$

$$\frac{\partial \hat{P}(T)}{\partial x_i} = \frac{\partial \hat{P}(T)}{\partial T} \cdot \frac{\partial T}{\partial x_i}$$

where $\hat{P}(T)$ is the saturation vapor pressure, which is a function of temperature T

$$\frac{\partial P_v}{\partial x_i} = \phi \frac{\partial \hat{P}}{\partial T} \cdot \frac{\partial T}{\partial x_i} + \hat{P} \frac{\partial \phi}{\partial x_i} \quad [4C]$$

d) Suction pressure gradient in liquid conduction term: $\frac{\partial P_s}{\partial x_i}$

Suction pressure can be expressed as a function of temperature and relative humidity using

Keleve's equation: $P_s(T, \phi) = -\frac{\rho_w RT}{M} \ln(\phi)$, where R is the universal gas constant and M is the

molecular weight of water molecule. Thus, an expression for suction pressure gradient as

function of temperature and relative humidity (Equation [4D]) can be obtained by making use of

the partial differentiation of Keleve's equation as follow:

$$\frac{\partial P_s}{\partial x_i} = \frac{\partial P_s}{\partial T} \cdot \frac{\partial T}{\partial x_i} + \frac{\partial P_s}{\partial \phi} \frac{\partial \phi}{\partial x_i}$$

$$\frac{\partial P_s}{\partial T} = -\frac{\rho_w R}{M} \ln(\phi)$$

$$\frac{\partial P_s}{\partial \phi} = -\frac{\rho_w RT}{M} \cdot \frac{1}{\phi}$$

$$\frac{\partial P_s}{\partial x_i} = -\frac{\rho_w R}{M} \left(\ln(\phi) \frac{\partial T}{\partial x_i} + \frac{T}{\phi} \frac{\partial \phi}{\partial x_i} \right) \quad [4D]$$

Finally, substituting Equation [4A], [4B], [4C] and [4D] into Equation [4] gives:

$$\underbrace{\Theta \frac{\partial \phi}{\partial t}}_{\frac{\partial w}{\partial t}} = \frac{\partial}{\partial x_i} \left(\delta_v \left[\underbrace{\phi \frac{\partial \hat{P}}{\partial T} \cdot \frac{\partial T}{\partial x_i} + \hat{P} \frac{\partial \phi}{\partial x_i}}_{\frac{\partial P_v}{\partial x_i}} - \rho_a V_i \underbrace{\left[\frac{0.622}{P_{atm}} \hat{P} \cdot \phi \right]}_{\omega} \right] + \frac{\partial}{\partial x_i} \left(D_l \frac{\rho_w R}{M} \left(\underbrace{\ln(\phi) \frac{\partial T}{\partial x_i} + \frac{T}{\phi} \frac{\partial \phi}{\partial x_i}}_{\frac{\partial P_v}{\partial x_i}} \right) - D_l \rho_w \bar{g} \right) \right)$$

This expression can be simplified to Equation [5], which represents the mathematical model implemented in this paper for the general case of non-isothermal moisture transfer through multilayered porous media.

$$\Theta \frac{\partial \phi}{\partial t} = \frac{\partial}{\partial x_i} \left(D_\phi \frac{\partial \phi}{\partial x_i} + D_T \frac{\partial T}{\partial x_i} \right) - \frac{\partial}{\partial x_i} (D_l \rho_w \bar{g} + \rho_a V_i C_c \hat{P} \cdot \phi) \quad [5]$$

$$\text{where: } D_\phi = \left(\delta_v \hat{P} + D_l \frac{\rho_w R T}{M \phi} \right) \quad D_T = \left(\delta_v \phi \frac{\partial \hat{P}}{\partial T} + D_l \frac{\rho_w R}{M} \ln(\phi) \right)$$

The above equation (Equation [5]) can be reduced for a simpler case where moisture transfer in a porous media is considered an isothermal process, and not considering either airflow or gravity

effects as: $\Theta \frac{\partial \phi}{\partial t} = \frac{\partial}{\partial x_i} \left(D_\phi \frac{\partial \phi}{\partial x_i} \right)$. If moisture content is used as a flow variable, the moisture

transfer equation can be written as: $\frac{\partial w}{\partial t} = \frac{\partial}{\partial x_i} \left(D_m \frac{\partial w}{\partial x_i} \right)$.

Combining these equations provides a relationship between the moisture conduction coefficient D_ϕ and moisture diffusivity D_m . This relation permits deducing both the liquid conduction coefficient and liquid conductivity from measurable quantities of moisture capacity, vapor permeability and moisture diffusivity.

$$D_\phi = D_m \cdot \Theta = \left(\delta_v \bar{P} + D_l \frac{\rho_w R T}{M \phi} \right) \quad D_l = \frac{M}{\rho_w R} \cdot \frac{\phi}{T} (D_m \cdot \Theta - \delta_v \bar{P})$$

2.2. Heat transfer

The conservation equation for internal energy and enthalpy are derived from the conservation equation of total stored energy, as given in Equation [6]. The total stored energy (E) of a system is the sum of internal energy (U), kinetic energy (KE) and potential energy (PE), $E = U + KE + PE$. The conservation equation for the total stored energy can be derived by considering a control volume, and accounting for the rate of change of stored energy in the control volume (term *I*), transport of energy in and out of the control volume by convection (term *II*) and diffusion (term *III*) as well as the work done by external forces at the surface of the control volume including viscous forces (term *IV*) and by gravity (body) force (term *V*) and heat source (or sink) (term *VI*) [15].

$$\underbrace{\frac{\partial(\rho e)}{\partial t}}_I + \underbrace{div(\rho V e)}_{II} = \underbrace{-div(j_q)}_{III} + \underbrace{div(\hat{\tau} V)}_{IV} + \underbrace{\rho(\vec{g} \cdot V)}_V + \underbrace{\dot{Q}}_{VI} \quad [6]$$

where e is energy per unit mass $\left(e = \frac{E}{m} = u + \frac{1}{2}|V|^2 + g \cdot x_i \right)$ and ρe is the energy per unit volume. After rearranging some mathematical expressions, the conservation equation for the total energy can be expressed in terms of enthalpy, h , as provided in Equation [7] (Kuo [15]).

$$\frac{\partial(\rho h)}{\partial t} + \text{div}(\rho V h) = -\text{div}(j_q) + \dot{Q}_s \quad [7]$$

where j_q is a diffusion term, which comprises heat transfer by conduction and enthalpy transport due to moisture transfer and \dot{Q}_s is a heat source (or sink) term. Rewriting the transient, convection and diffusion terms using mixture enthalpy (moisture, air and solid matrix), and subsequent simplification of Equation [7] yields the mathematical model, implemented in this paper, for transient heat transfer through porous media, Equation [8].

$$\rho_m C_{p_{eff}} \frac{\partial T}{\partial t} + \rho_a (C_{p_a} + \omega C_{p_v}) \text{div}(VT) + \text{div}(-\lambda_{eff} \text{grad}(T)) = \dot{m}_c h_{fg} + \dot{m}_c T (C_{p_v} - C_{p_l}) + \dot{Q}_s \quad [8]$$

where $C_{p_{eff}}$ and λ_{eff} are the effective specific heat capacity and thermal conductivity (which take moisture effect into account), respectively, and $\dot{m}_c = \text{div}\left(\delta_v \frac{\partial P_v}{\partial x_i}\right) - \rho_a \text{div}(V\omega)$ is the amount of moisture condensation/evaporation in kg/s.

2.3. Airflow through porous media

Airflow through a porous media can be expressed by using Poiseuille's law of proportionality [16], which relates the pressure gradient to flow velocity (Equation [9]).

$$V = -\frac{k_a}{\mu} \text{div}(P) \quad [9]$$

In building physics applications, air is considered incompressible due to the very low airflow speeds, and low pressure and temperature changes that are encountered in practice. Consequently, the conservation equation for air mass balance is given by Equation [10].

$$\text{div}(\rho_a V) = 0 \quad [10]$$

Combing the mass balance, given in Equation [10], and momentum balance, provided in Equation [9], gives Equation [11], which is implemented in this paper to compute airflow velocities through building enclosures.

$$-\text{div}(\delta_a \text{div}(P)) = 0 \quad [11]$$

where $\delta_a = \rho_a \frac{k_a}{\mu}$ (air permeability).

3. NUMERICAL TOOL FOR TRANSIENT HAM ANALYSIS

The mathematical models implemented in this paper are Equation [5], [8], and [11] for moisture, heat and air transport through multilayered porous media, respectively. The solution to the air balance equation, flow through a porous media with perfect contact between adjacent layers, is relatively straightforward if the air permeability of the medium is assumed to be constant, which is a generally the case in building physics applications. In this instance, Equation [11] is solved independently for the pressure distribution in the medium of a given boundary pressure condition. Subsequently, Equation [9] is used to calculate the airflow velocity field. The known velocity field will then be used in the convection transport terms of moisture and energy equations, Equation [5] and [8] respectively.

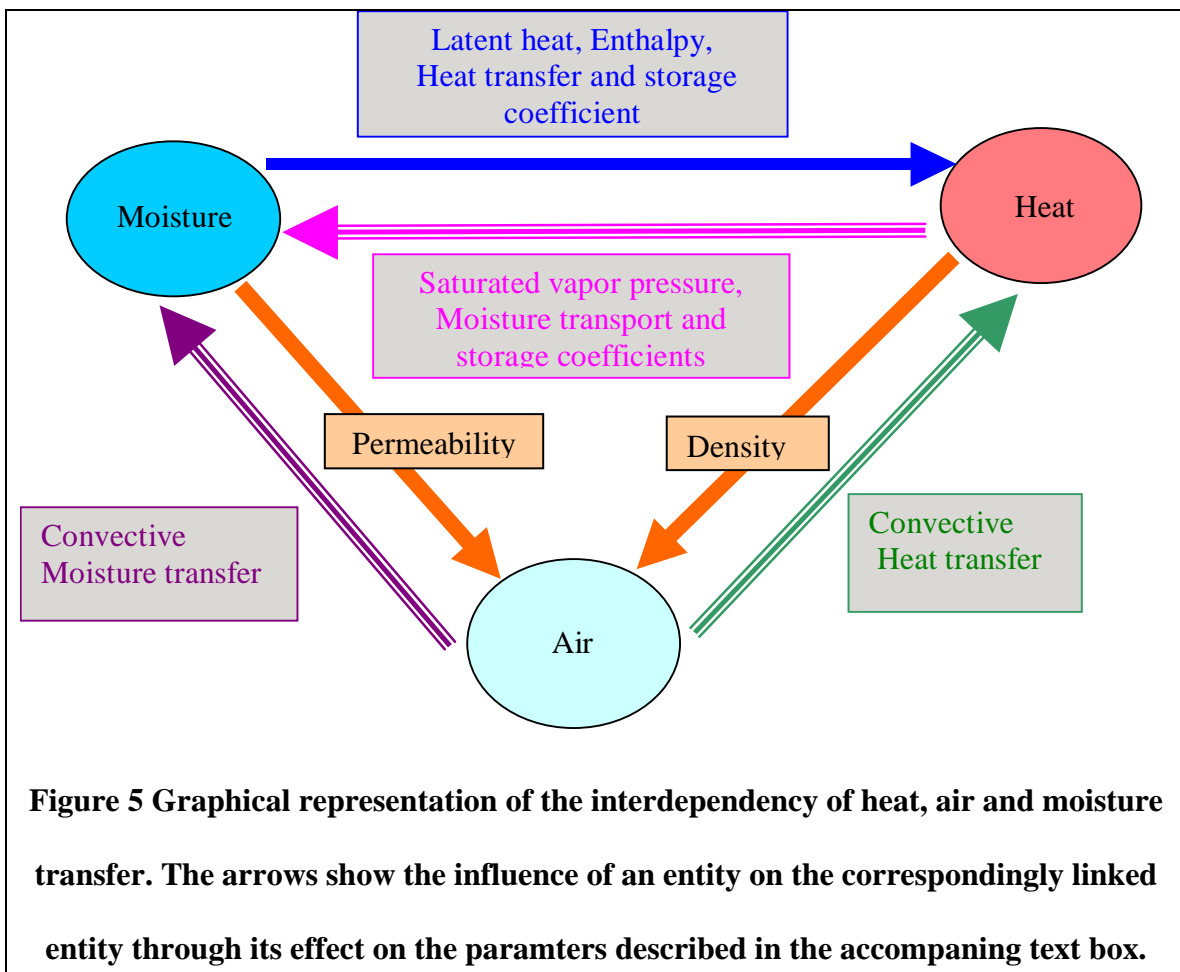


Figure 5 shows a graphical representation of the interdependency of heat, air and moisture transfer in a porous media. The heat and moisture balance equations (Equation [8] and [5], respectively) are highly coupled in a way that the heat transfer solution depends on the moisture balance solution and vice versa. Temperature and moisture content can affect the air density and permeability of the porous media, and in turn the mechanisms of convective heat and moisture transfer. In the heat balance equation, Equation [8], the thermal storage and transfer properties of materials (effective heat capacity, Cp_{eff} , and apparent thermal conductivity, λ_{eff}) as well as the local heat source/sink (associated with moisture phase change, \dot{m}_c) depend on the moisture state of the domain. On the other hand, the temperature fields affect the moisture transfer process since the temperature gradient is one of the moisture driving forces as indicated in the moisture balance equation (Equation [5]). Moreover, the vapor permeability, moisture transfer coefficients (D_ϕ and D_T) and saturated vapor pressure, which are important parameters in the moisture balance equation, are temperature dependent. In addition to the strong coupling between the heat and moisture balance equations, the equations themselves are highly non-linear due to the fact that neither the transfer nor the storage coefficient of the respective balance equations are constants but are functions of the corresponding driving potentials.

For example, the moisture and heat transfer properties of a load bearing material [17], which is used in one of the HAMSTAD² benchmark exercises, are presented in Figure 6 and Figure 7, respectively. Figure 6 shows the non-linearity of the relationship of the sorption capacity and vapor permeability with relative humidity as well as the liquid diffusivity with moisture content. As moisture content (or relative humidity) increases these properties exhibit more non-linear behavior depicting a high increase in sorption capacity, decreases in vapor transport and

² HAMSTAD stands for Heat, Air and Moisture Standard Development.

significant increase in liquid water transport. Likewise, Figure 7 shows the moisture dependency of the thermal properties for this same material; the heat storage capacity and thermal conductivity of the material increases with moisture content.

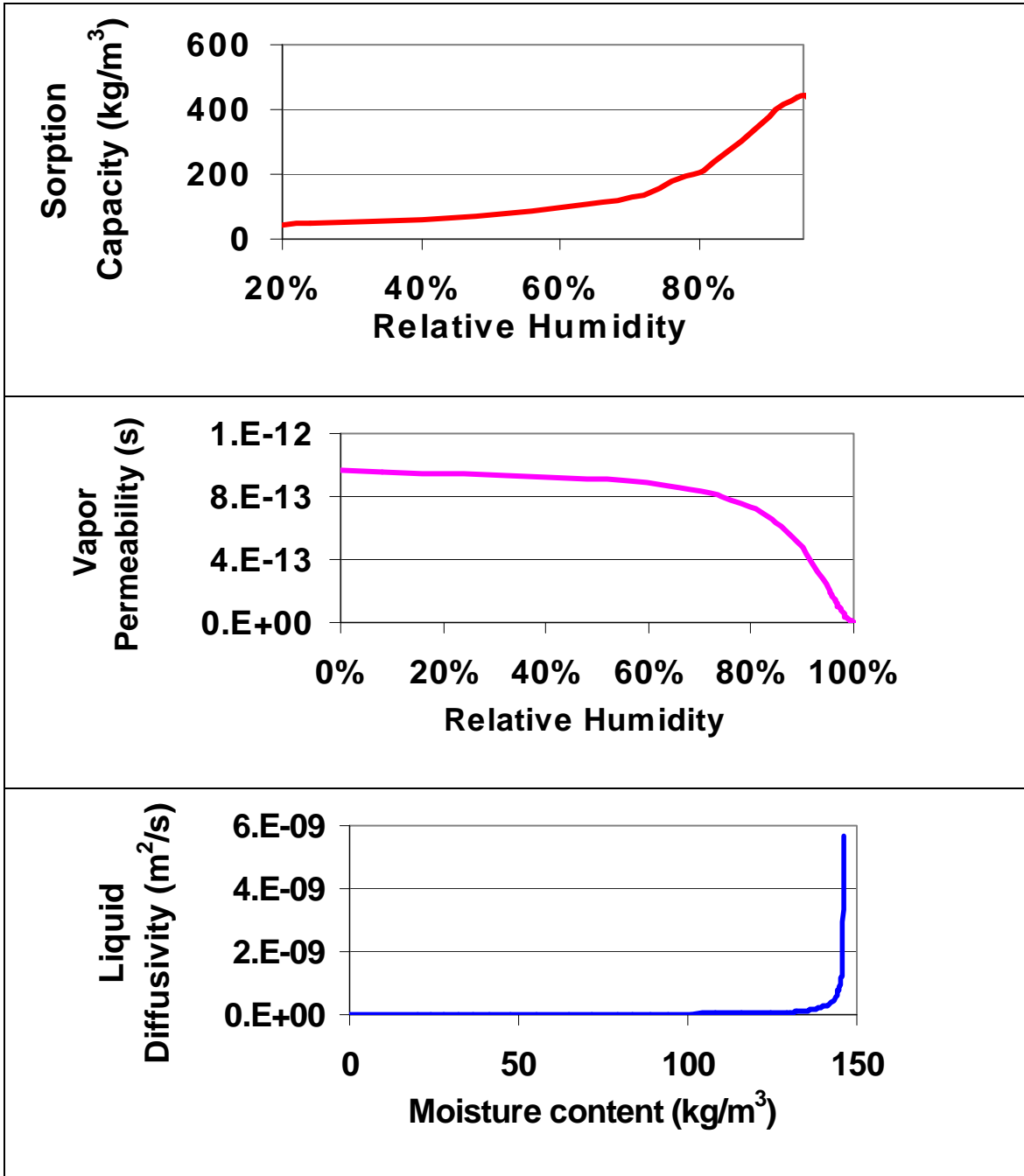


Figure 6 Typical moisture transport properties curves. As moisture content increases the transport properties exhibit non-linear behavior.

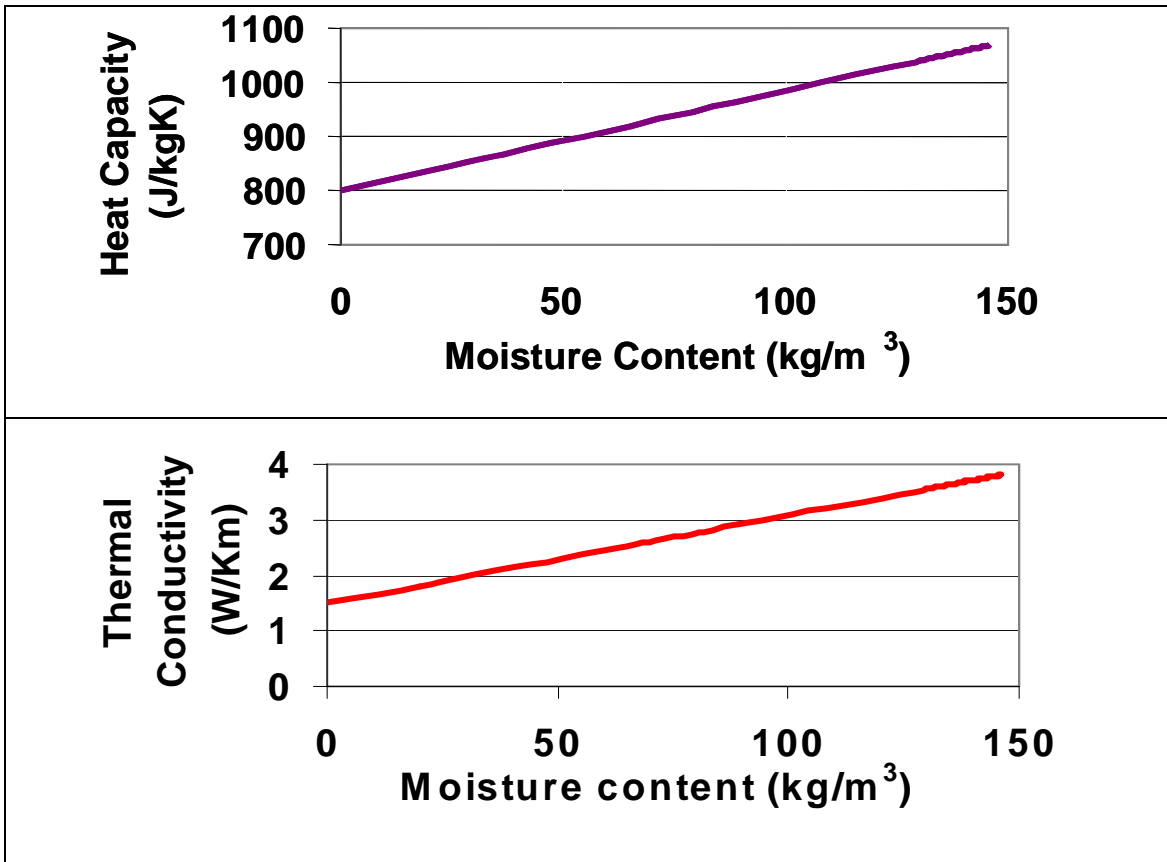


Figure 7 Typical thermal properties as a function of moisture content.

Numerical tool

To obtain the temperature and relative humidity field across the computational domain (multilayered building envelop component), the coupled and nonlinear partial differential equations (PDEs) need to be solved simultaneously. Here, a finite-element based computational tool called COMSOL Multiphysics³ and MatLab⁴ were used to solve these equations. In addition to a solver, COMSOL Multiphysics has a graphical user interface (GUI) to create computational domain geometry, an automated and user controlled mesh generator, and it also has an integrated

³ COMSOL Multiphysics: <http://www.comsol.com/>

⁴ Mathworks <http://www.mathworks.com>

post processing capability for plotting, interpolating and integrating simulation results. The COMSOL Multiphysics computational tool has a library of predefined models to solve familiar engineering problems such as convection diffusion, fluid dynamics, heat transfer and other problems. It also has a provision to apply equation based modeling techniques, referred as “PDE Modes”, for solving problems that may not be solved by the standard modules. Using this numerical technique, the developer formulates the PDEs that govern the physical phenomena, and solves them using the built-in solver.

In this paper, the three-coupled transient HAM equations were simultaneously solved using the COMSOL Multiphysics time-dependent solver. The solver is based on an explicit scheme with variable time stepping. The user can predefine the maximum time step so that it matches with the boundary conditions change periods.

4. BENCHMARKING OF THE TRANSIENT COUPLED HAM MODEL

In this section, the newly developed transient coupled HAM model is benchmarked against published test cases. This is an important step that must first be carried out before integrating it with an indoor model to develop the whole building hygrothermal model, which is presented in the second part of this paper.

The test cases comprise an analytical verification, comparisons with other models, and validation of simulation results with experimental data. Judkoff and Neymark [18] recommend these three classes of model evaluation methods to test whether the mathematic models that are incorporated in the numerical tool describe the physical processes of interest adequately. Here, two of the five benchmarking exercises that were designed under the European HAMSTAD project and a drying experiment carried out by Maref et al. [19] are presented as they cover the

three categories of model test cases. The HAMSTAD project was initiated to develop standard test cases, by which the accuracy of the existing and newly developed hygrothermal models should be evaluated [17]. The complete benchmarking exercises that are undertaken to test the model are reported in Tariku [20].

4.1. Analytical verification -- HAMSTAD Benchmark Exercise #2

In this benchmark exercise, a schematic of which is given in Figure 8, the isothermal drying process of a relatively wet 200 mm thick homogeneous layer structure is considered. The initial hygrothermal conditions of the structure are 20°C and 95% relative humidity. The level of relative humidity of the surrounding environment is changed so that the structure dries out by moisture redistribution and release to the surroundings. The top (exterior) and bottom (interior) surfaces of the structure are exposed to 45% and 65% relative humidity, respectively, while the temperature is kept constant at 20°C. The heat and mass transfer coefficients for both surfaces are 25 W/m²K and 1E-3 s/m, respectively. The material properties of the structure are given in Table 1 below. This benchmark exercise is a test case that has an analytical solution. This is possible due to the fact that the drying process is isothermal, and the boundary conditions and hygrothermal properties of the material are assumed to be constant. The full description of this benchmark exercise is given in Hagentoft [17].

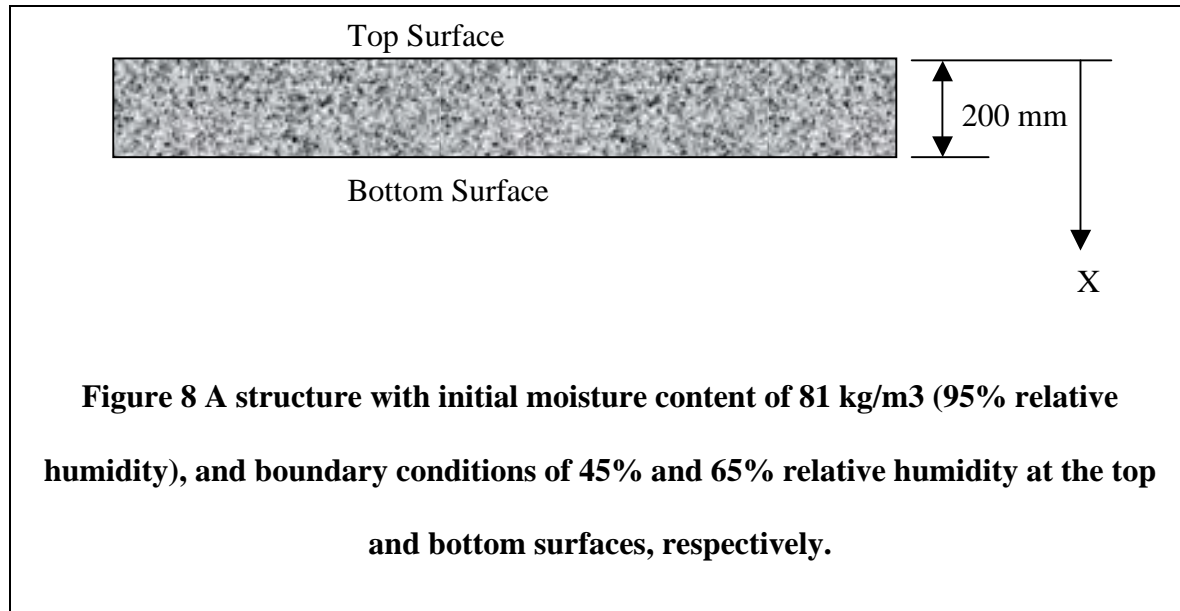


Table 1 Hygrothermal properties of the monolithic structure

Sorption isotherm	$w = \frac{116}{\left(1 - \frac{1}{0.118} \ln(\phi)\right)^{0.869}} \text{ kg/m}^3$
Vapor diffusion	10^{-15} s
Moisture diffusivity	$6 \times 10^{-10} \text{ m}^2/\text{s}$
Thermal conductivity	0.15 W/m K
Heat capacity	$4.2 \times 10^5 \text{ J/m}^3 \text{ K}$

The accuracy of the numerical model in simulating the drying process of the structure is verified by comparing the model results with the analytical solutions, which are provided in the HAMSTAD project report. The transient moisture profiles (moisture content in kg/m^3) across the structure, which result due to the continuous release of moisture from the structure to the surrounding through its boundary surfaces, are used as verification parameters. Figure 9 shows the initial moisture content and the moisture distribution across the structure at 100, 300 and 1000 hours. In this and the following figures, the simulation results of the model are designated as “HAMFit”. The moisture distributions at the top, middle and bottom sections of the structure at 1000 hours are presented in Figure 10, Figure 11 and Figure 12, respectively. As can be seen in these figures, the newly developed model produced excellent results that clearly show high degree of agreement with the analytical solutions.

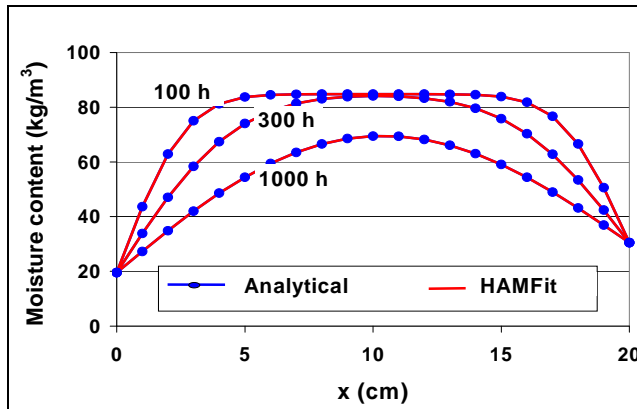


Figure 9 Moisture profiles of the structure at 100, 300 and 1000 hours from the initial moisture content of 80.8 kg/m^3 .

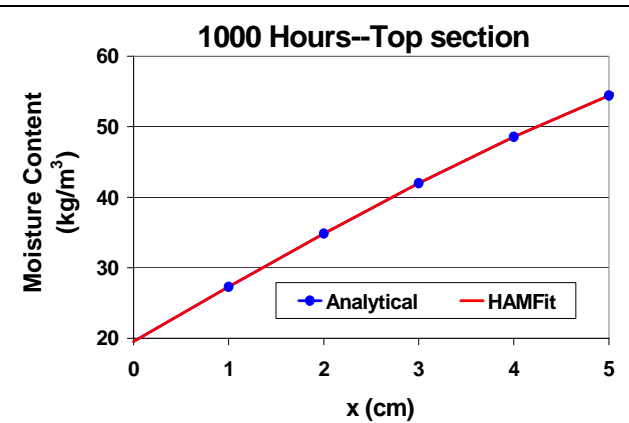


Figure 10 Moisture distribution of the top section of the structure at 1000 hours.

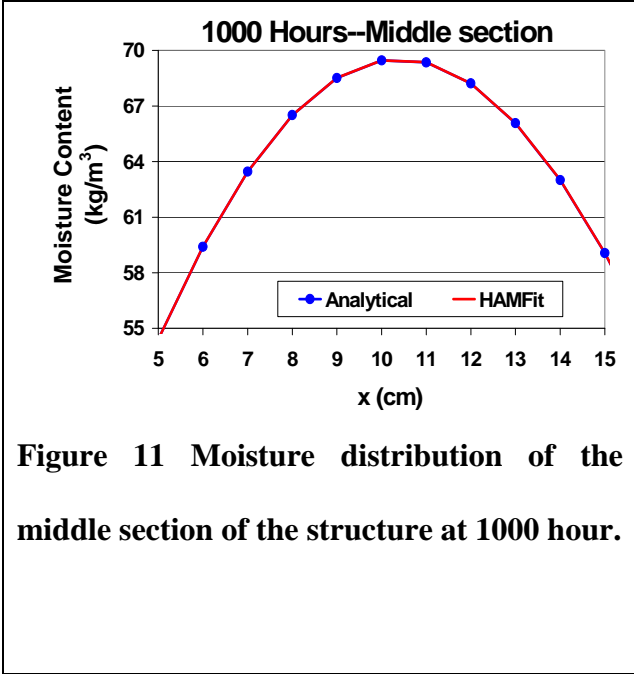


Figure 11 Moisture distribution of the middle section of the structure at 1000 hour.

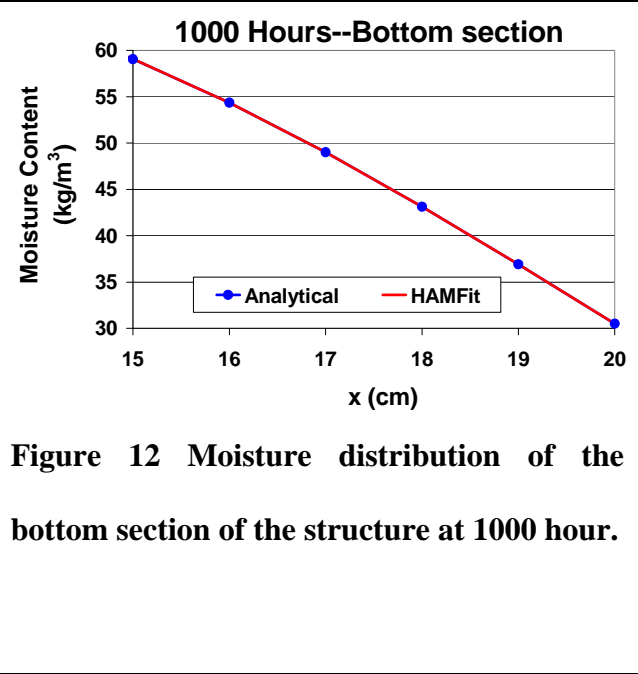


Figure 12 Moisture distribution of the bottom section of the structure at 1000 hour.

4.2. Comparative analysis —HAMSTAD Benchmark Exercise #4

In this benchmark exercise, the dynamic responses of the HAM model for a well-defined heat and moisture transfer problem are compared with other models’ simulation results. The prerequisite for such type of comparative analysis is that all model input parameters including geometrical representation, dimensions, initial conditions, internal and external boundary conditions, and material properties of the building envelope systems have to be prescribed and consistently used by all participating models. The full description of the benchmark exercise can be found in Hagentoft [17]. Here, a brief description of the problem, input parameters and results are presented.

The test case deals with heat and moisture transfer in a two-layer wall system exposed to realistic internal and external boundary conditions. The wall system is composed of a load-bearing layer on the exterior, and finishing layer on the interior of the wall system. The load-

bearing layer is 100 mm thick and has a density of 2050 kg/m^3 and specific heat capacity of 840 J/(K.kg) ; the finishing layer has a thickness of 20 mm, density 790 kg/m^3 and specific heat capacity of 870 J/(K.kg) . Realistic time dependent boundary conditions that are applied at the external and internal surfaces of the wall are shown in Figure 13. The variable heat and moisture loads on the exterior surface due to solar radiation and rain are represented by equivalent outdoor temperature (shown on the top figure) and wind-driven rain flux (shown on the last figure), respectively. The time dependent indoor moisture load that may be related to occupant activity, is represented by variable indoor vapor pressure (shown on the middle figure). The outdoor air temperature and vapor pressure, as well as the indoor air temperature are held constant with values of 10°C , 1150 Pa , and 20°C respectively. This test case is more challenging [21] as it involves severe climatic load that causes surface condensation on the exterior surface due to nighttime cooling (low equivalent temperature), and frequent occurrences of wetting and drying of the wall due to the alternating rain and solar radiation loads. Moreover, the problem involves rapid rainwater absorption at the interfaces and high rate of moisture movement within the layers due to the extremely high liquid water absorption property of the load-bearing layer.

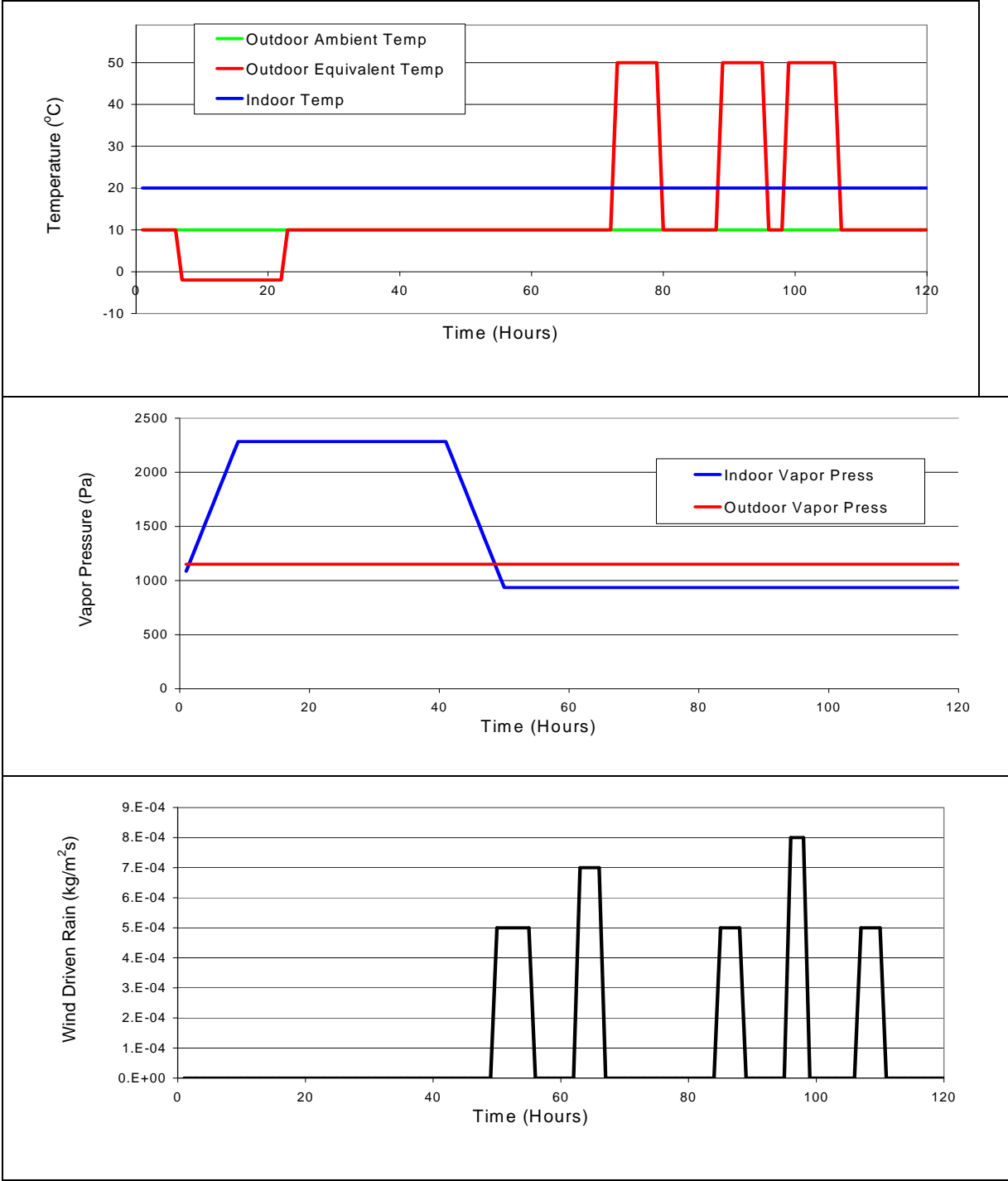


Figure 13 Boundary conditions imposed on the indoor and outdoor surfaces

The initial hygrothermal conditions of the two layers are 20°C and 40% temperature and relative humidity, respectively. The mass transfer coefficients of the interior and exterior surfaces are 3E-8 and 2E-7 s/m, respectively. The heat transfer coefficients for the corresponding

surfaces are 8 and 25 W/(m².K), respectively. For comparison purposes, the model simulation results (designated as “HAMFit”) are superimposed on the corresponding six HAMSTAD project participants’ solutions. Figure 14 shows the transient surface moisture contents and temperatures of the outer and inner surfaces of the wall for the entire simulation period. The moisture content and temperature profiles of the wall system after 96 hours are presented in Figure 15. As can be seen in these figures, the simulation results of the model are in very good agreement with the other six models’ solutions (labeled 1 to 6). In whole building hygrothermal modeling, the coupling of building enclosure and indoor environment is through interior surfaces, and therefore, it is important to accurately predict the hygrothermal states of these surfaces to obtain useful results.

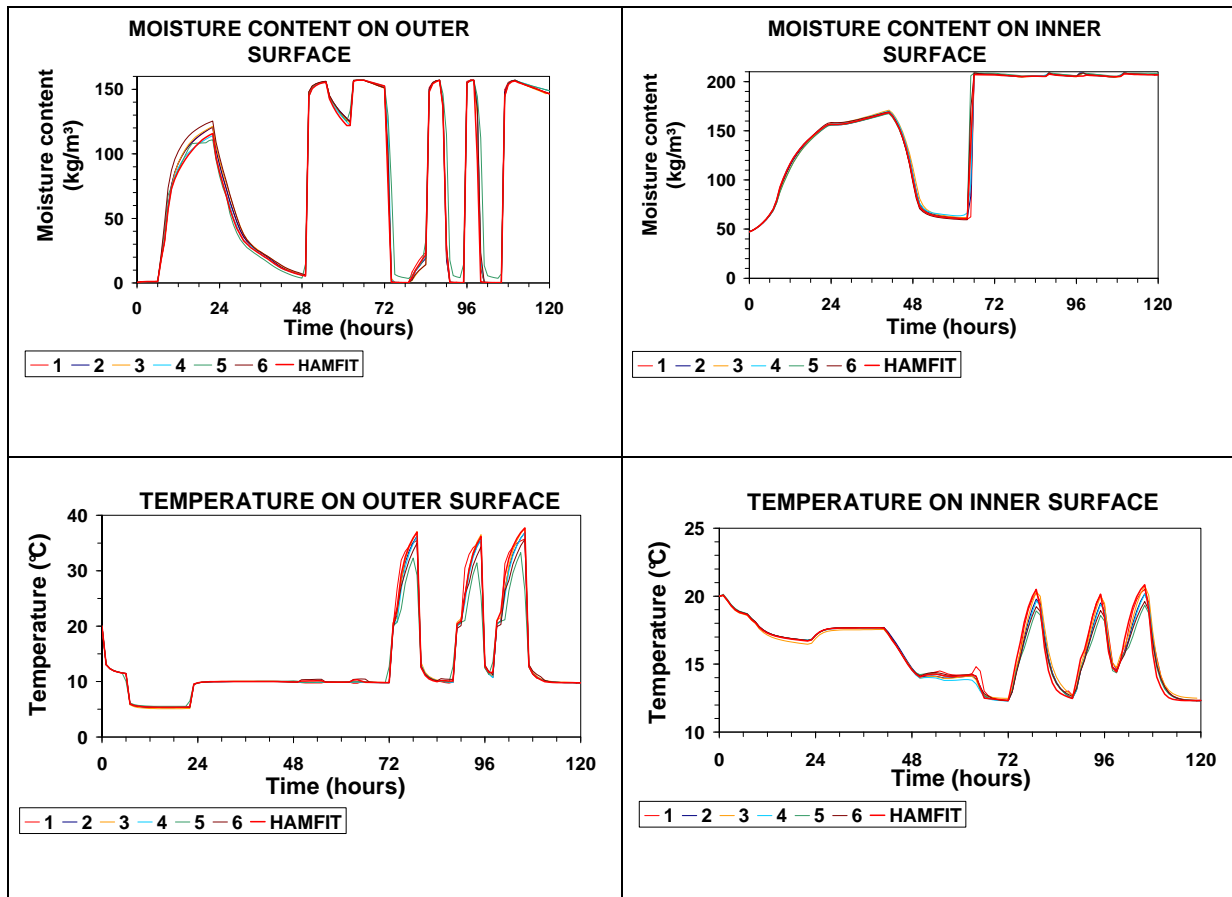


Figure 14 The transient surface moisture content and temperature of the outer and inner surfaces of the wall for the entire simulation period

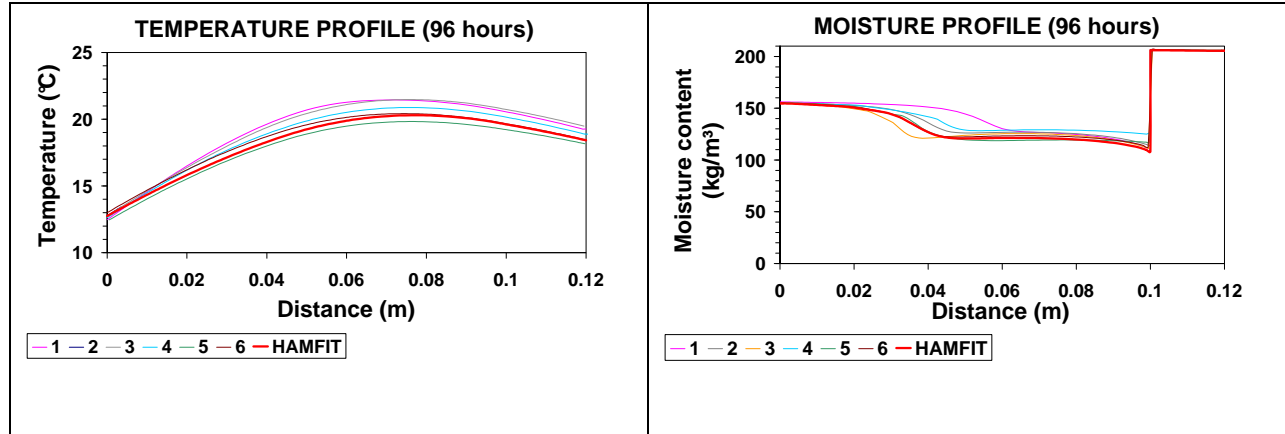


Figure 15 The moisture content and temperature profiles of the wall system at 96 hours.

4.3. Experimental validation—Laboratory controlled experiment

In this section, a drying experiment carried out by Maref et al. [19] is used for validation and testing of the model. The model’s prediction is compared with this laboratory controlled measured data. In fact, the main objective of Maref’s experiment was to provide measured data by which building envelope models could be tested and validated. The experiment was done on full-scale size wall having equal height and width of 2.4 m. The wall system is comprised of a wood frame, sheathing board (11.5 mm thick OSB) and vapor barrier (polyethylene sheet) that are installed on the outside and interior surfaces of the frame, respectively. The cavity between the vertical wood studs is filled with glass fiber insulation. The experiment was designed to measure the drying rate of a wetted sheathing board (OSB) as it is exposed to controlled indoor and outdoor boundary conditions. At the beginning of the experiment, the equilibrium moisture content of the wetted OSB was 330 kg/m^3 , which is equivalent to 99.6% relative humidity. This initial moisture condition was attained by carrying out a preconditioning process that involved:

soaking the OSB in a water bath, and thereafter, wrapping it up with polyethylene sheet to allow moisture redistribution across the thickness of the panel. As part of the experimental setup, all surfaces of the wood frame were coated with vapor tight paint to restrict moisture exchange with the surroundings including the OSB. Furthermore, the edges of the OSB were sealed to prevent moisture loss through these surfaces. These preliminary actions suggest that the drying process is one-dimensional and takes place through the OSB planer surfaces. During the experiment, any weight loss recorded by the weighing system was interpreted as moisture loss (drying) of the OSB to the outdoor environment. The basis for this assumption are the following: 1) the weight of the wood-frame remains the same since its moisture exchange with the surrounding is restricted by the paint; 2) moisture accumulation in the insulation is insignificant due to its non-hygroscopic nature; 3) condensation on the exterior surface of the polyethylene sheet is insignificant since the indoor and outdoor temperature conditions are nearly the same.

The OSB used in this experiment had a density of 650 kg/m^3 , thermal conductivity of $9.41\text{E-}02 \text{ W/(m.K)}$ and specific heat capacity of 1880 J/(kg.K) . Its moisture storage and transport properties that include the sorption isotherm, vapor permeability and liquid diffusivity are known from the experimental study. The density, thermal conductivity, heat capacity and vapor permeability of the glass fiber insulation are 11 kg/m^3 , $3.66\text{E-}02 \text{ W/(m.K)}$, 1256 J/(kg.K) and $1.30\text{E-}10 \text{ kg/(s.Pa.m)}$, respectively. Since the insulation is non-hygroscopic its moisture storage capacity is very low, and therefore neglected in the modeling. Moreover, due to its capillary non-active nature, the liquid water transport property was set to zero. The vapor permeability of polyethylene sheet is $2.29\text{E-}15 \text{ kg/(s.Pa.m)}$. As far as hygrothermal modeling is concerned, vapor permeability is the most important hygrothermal property of the polyethylene sheet; the remaining properties including moisture storage, thermal storage, liquid permeability and

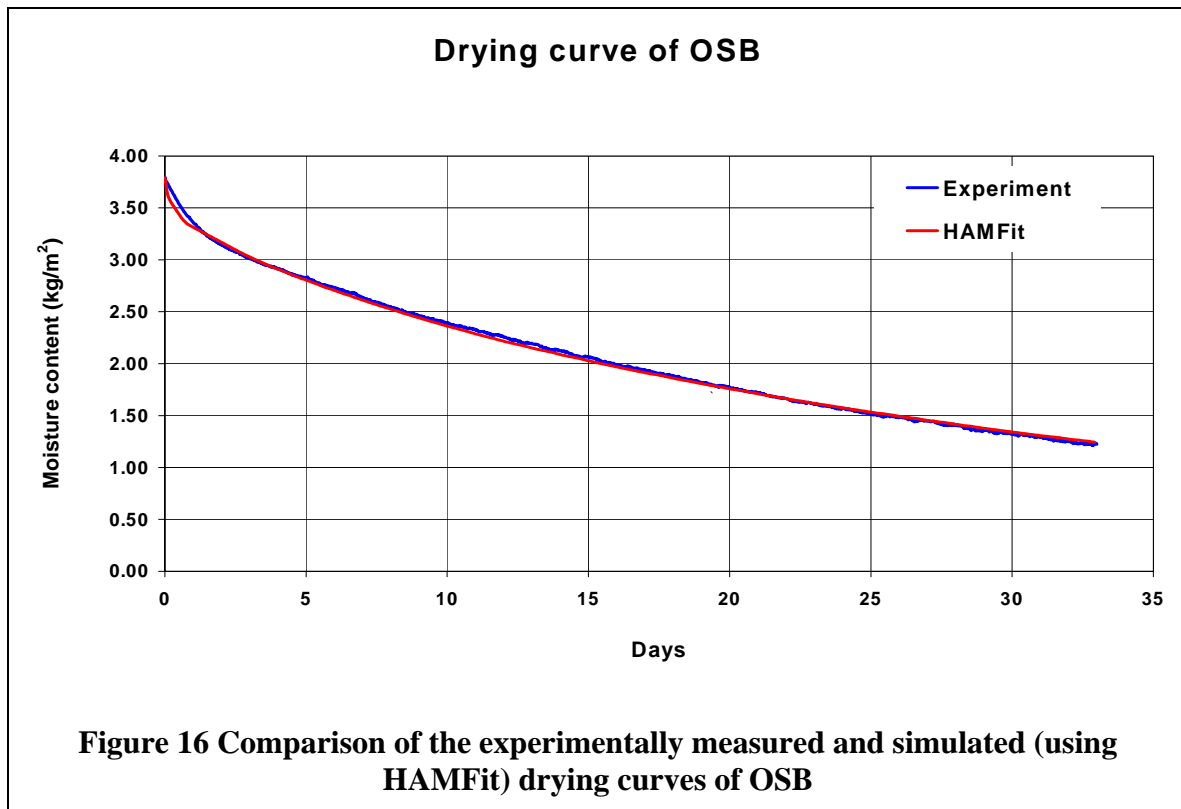
thermal resistance values were set to zero. Since the polyethylene sheet was directly exposed to the indoor boundary condition, it was modeled as a surface vapor resistance rather than as a layer.

The two remaining, and essential input data for benchmarking of hygrothermal models using laboratory-controlled experiments are: initial and boundary conditions. The initial equilibrium moisture content of the OSB was 330 kg/m^3 , and the corresponding relative humidity (from sorption isotherm curve) was 99.6%. In the simulation, the initial moisture content was assumed to be uniform across the OSB thickness. This is based on the step taken during the preconditioning process, more specifically, wrapping the wetted OSB with a polyethylene sheet to allow moisture redistribution. The initial temperature condition of the wall system was assumed to be 25°C and uniform across the thickness. The boundary conditions to which the wall system was exposed were controlled and measured over the course of the experiment. The temperature and relative humidity conditions of the outdoor environment were fairly constant at 25°C and 25%, respectively. For most of the time during the experiment, the temperature difference across the wall was between $1\text{--}2^\circ\text{C}$. This small temperature difference coupled with the presence of insulation in the cavity makes the drying process nearly an isothermal process. The indoor relative humidity was generally higher and more variable than the outdoor relative humidity (with a mean value of 40%). However, its effect on the drying process was very limited due to the presence of the polyethylene sheet, which essentially creates an interior adiabatic boundary condition for moisture transfer.

In the simulation, the mass transfer coefficients are determined from the heat transfer coefficients using Lewis relation [11]. Since the experiment is carried out in the indoor environment, a heat transfer coefficient that is recommended in the IEA/Annex 24 [22] for

interior flat surface $8 \text{ W}/(\text{m}^2\text{K})$ is adopted for both interior and exterior surfaces. Based on Lewis relation, the mass transfer coefficients for the exterior surface is determined to be $5.80\text{E-}8 \text{ s/m}$. $1.53\text{E-}11$ and $5.80\text{E-}8 \text{ s/m}$, respectively. The effective mass transfer coefficient of the interior surface was $1.53\text{E-}11 \text{ s/m}$, which is calculated by superimposing the vapor resistance of polyethylene sheet on the vapor flow resistance created by the moist-air boundary layer.

In Figure 16 the simulation result for the OSB drying curve derived from the model (HAMFit) is superimposed on the laboratory results, which depict the transient moisture content of the OSB at different times over the drying period. As can be seen in the figure, the model prediction is in excellent agreement with the experimental results for the entire drying period. During this period, the OSB lost 2.5 kg of moisture per square meter of OSB. The average moisture content of the OSB by weight was reduced from 51% (initial state) to 16% (end of experiment).



5. CONCLUSION

The thermal and moisture dynamic responses of building enclosures, essential inputs for whole building hygrothermal models, have strong impact on the overall performance of the building. This is due to the fact that the moisture stored in the structure affects the indoor humidity and energy flow across the structure, and thereby HVAC equipment size. Moreover, building enclosures can have significant influence on the indoor humidity level depending on the moisture buffering capacity of the interior lining materials. The dynamic influences of building enclosures on the indoor environment and HVAC systems can be captured by using a transient model that handles coupled heat, air and moisture transfer through multilayered porous media.

In this paper, a transient heat, air and moisture transfer model is developed based on basic conservation of mass and energy equations. The governing partial-differential equations (PDEs) of the three transport phenomena are coupled and solved simultaneously for temperature, relative humidity and pressure. The model accommodates non-linear transfer and storage properties of materials, moisture transfer by vapor diffusion, capillary liquid water transport and convective heat and moisture transfer through multi-layered porous media. The PDEs are derived in such a way that each PDE is described with a single driving potential, which is continuous across the interfaces of adjoining materials. Consequently, an equation-based modeling technique, which requires less time of implementation and provides high degree of transparency and flexibility of modeling, is used for solving the coupled PDEs. The transient HAM model is successfully benchmarked against three published test cases. The test cases are comprised of an analytical verification, comparisons with other models and validation of simulation results with experimental data. The good agreement obtained with the respective test cases suggest that the model development and implementation are satisfactory, and therefore, can be further coupled

with an indoor model to create a whole building hygrothermal model. The development and benchmarking of a holistic model that utilizes the transient model developed in this paper as one of its building block will be presented in subsequent paper.

ACKNOWLEDGEMENTS

The authors thank Dr. Wahid Maref for providing the experimental data used in the third benchmark exercise.

6. REFERENCES

- [1] R. El Diasty, P. Fazio and I. Budaiwi, Modelling of Indoor Air Humidity: The Dynamic Behavior within an Enclosure. *Energy and Buildings*, Vol. 19, pp.61-73 (1992).
- [2] R. Jones, Indoor Humidity Calculation Procedures. *Building Services Engineering Research and Technology*, Vol. 16 (3), pp.119-126 (1995).
- [3] C. Simonson, M. Salonvaara and T. Ojanen, Heat and Mass Transfer Between Indoor Air and a Permeable and Hygroscopic Building Envelope: Part 1 – Field Measurements. *Journal of Thermal Envelope and Building Science*, Vol. 28 (1), pp. 63-101 (2004).
- [4] C. Simonson, M. Salonvaara and T. Ojanen, Heat and Mass Transfer Between Indoor Air and a Permeable and Hygroscopic Building Envelope: Part II – Verification and Numerical Studies. *Journal of Thermal Envelope and Building Science*, Vol. 28 (2), pp. 161-185 (2004).
- [5] A. TenWolde, Mathematical Model for Indoor Humidity in Houses during Winter, *Proceedings of Symposium on Air Infiltration, Ventilation and Moisture Transfer*, Washington DC: Building Thermal Envelope Coordinating Council (1988).

- [6] J.E. Christian, Moisture Sources. Moisture Control in Buildings, ASTM Manual Series: MNL 18, pp. 176-182 (1994).
- [7] A. TenWolde and C.L. Pilon, The Effect of Indoor Humidity on Water Vapor Release in Homes. *Proceedings of Thermal Performance of the Exterior Envelopes of Whole Buildings X International Conference*. Dec. 2-7, Clearwater, FL (2007).
- [8] F. Tariku and M. K. Kumaran, Hygrothermal Modeling of Aerated Concrete Wall and Comparison With Field Experiment. *Proceeding of the 3rd International Building Physics /Engineering Conference*, August 26-31, Montreal, Canada, pp 321-328 (2006).
- [9] F. Tariku, S. Cornick and M. Lacasse, Simulation of Wind-Driven Rain Effects on the Performance of a Stucco-Clad Wall. *Proceedings of Thermal Performance of the Exterior Envelopes of Whole Buildings X International Conference*. Dec. 2-7, Clearwater, FL (2007).
- [10] N. Mendes, F.C. Winkelmann, R. Lamberts, and P.C. Philippi, Moisture Effects on Conduction Loads, *Energy and Buildings*, Vol. 35, pp. 631-644 (2003).
- [11] ASHRAE Handbook of Fundamentals, American Society of Heating, Refrigeration, and Air-Conditioning Engineers, Atlanta (2005).
- [12] H. Kuenzel, A. Karagiozis and A. Holm, A Hygrothermal Design Tool for Architects and Engineers, *Moisture Analysis and Condensation Control in Building Envelopes*, ASTM Manual series 50: Chapter 9 (2001).
- [13] C-E, Hagentoft, Heat, Air and Moisture Transfer through New and Retrofitted Insulated Envelope Parts, *IEA Annex 24 HAMTIE*, Final Report, Vol.5, Task 5: Performances and Practice, ISBN 90-75741-04-9 (1996).
- [14] C-E, Hagentoft, C. Building Physics Fundamentals, *Report R-97:1*, Department of Building Physics, Chalmers University of Technology, Sweden (1997).

- [15] K. Kuo, Principles of Combustion, *Published by John Wiley & Sons Inc.* ISBN 0-471-09852-3 (1986).
- [16] H. Hens, *Building Physics-Heat, Air and Moisture, Fundamentals and Engineering Methods with Examples and Exercises*, Published by Ernst & Sohn A Wiley Com. ISBN 978-3-433-01841-5. (2007).
- [17] C-E. Hagentoft, HAMSTAD – Final report: Methodology of HAM-modeling, *Report R-02:8*. Gothenburg, Department of Building Physics, Chalmers University of Technology (2002).
- [18] R. Judkoff and J. Neymark, Building Energy Simulation Test (BESTEST) and diagnostic method. *NREL/TP-472-6231*. Golden, CO National Renewable Energy Lab (1995).
- [19] W. Maref, M. Lacasse, K. Kumaran and M.C. Swinton, Benchmarking of the advanced hygrothermal model-hygIRC with mid-scale experiments. *eSim 2002 Proceedings*, University of Concordia, Montreal, pp. 171-176 (2002).
- [20] F. Tariku, Whole Building Heat and Moisture Analysis, Ph.D. Thesis, Concordia University, Montreal, Canada (2008).
- [21] C-E. Hagentoft, A. Kalagasidis, B. Adl-Zarrabi, S. Roels, J. Carmeliet, H. Hens, J. Grunewald, M. Funk, R. Becker, D. Shamir, O. Adan, H. Brocken, K. Kumaran and R. Djebbar, Assessment Method of Numerical Prediction Models for Combined Heat, Air and Moisture Transfer in Building Components: Benchmarks for One-dimensional Cases. *Journal of Thermal Envelope and Building Science*. Vol. 27 (4), pp. 327-352 (2004).
- [22] C. Sanders, Heat, Air and Moisture Transfer Through New and Retrofitted Insulated Envelope Parts, *IEA Annex 24 HAMTIE*, Final Report, vol.2, Task2: Environmental conditions, K.U Leuven, Belgium (1996).

